# Probing the linear and nonlinear excitations of Bose-condensed neutral atoms in a trap

P. A. Ruprecht,[1] Mark Edwards,[2,3] K. Burnett,[1,3] and Charles W. Clark[3]
[1]*Clarendon Laboratory, Physics Department, University of Oxford, Oxford OX1 3PU, United Kingdom*
[2]*Department of Physics, Georgia Southern University, Statesboro, Georgia 30460-8031*
[3]*Electron and Optical Physics Division, Physics Laboratory, National Institute of Standards and Technology, Gaithersburg, Maryland 20899*
(Received 3 August 1995; revised manuscript received 22 April 1996)

We investigate the response of a Bose-Einstein condensate of trapped, neutral atoms to weak and strong sinusoidal perturbation of the trapping potential both by solving the Bogoliubov equations and by direct integration of the time-dependent, driven Ginzburg-Pitaevskii-Gross equation. We find that the distortion of the condensate is maximal when the frequency of the perturbation equals one of the mode positions of the condensate's excitation spectrum. On resonance, the condensate exhibits a strong nonlinear response that can be used as a clear signature of the mode frequency in an experiment where the trap potential is weakly perturbed. For strong driving, we find evidence for an array of nonlinear effects such as harmonic generation and frequency mixing. These phenomena are the matter-wave analogs of conventional nonlinear optics and should be straightforward to study in evaporatively cooled samples of alkali-metal atoms. [S1050-2947(96)03009-0]

PACS number(s): 03.75.Fi, 05.30.Jp, 67.90.+z

## I. INTRODUCTION

Now that Bose-Einstein condensation (BEC) has been achieved in magnetic, alkali vapors [1–3], we look forward to the prospect of experimentally probing the properties of these recently developed macroscopic quantum systems. This prospect provides strong motivation for the development of theoretical descriptions of condensate properties. One important issue for such theory is the vibrational excitation spectrum of the condensate [4]. Below the condensation point, it is the modification of this spectrum, that is, the modification of the system's response to perturbations, that leads to such well-known effects as superfluidity. As the vibrational excitations of the condensed gas can differ substantially from those of an uncondensed atomic vapor, they may well provide a means to determine the presence and properties of a trapped condensate. The linear excitation spectrum for a homogeneous, weakly interacting condensate at zero temperature was derived many years ago by Bogoliubov [5]. This method was extended by Pitaevskii [6] and the finite temperature version described for inhomogeneous condensates by Fetter [7].

A key feature of the experiments in which BEC has, to date, been reported [1–3] is the ability, through the use of forced evaporative cooling, to control the condensate fraction of the system. It is therefore possible to cool the system to the point where the number of condensate atoms far exceeds the number of thermal atoms. In this case, the system temperature is well below the condensation point and the Bogoliubov approximation will apply. Under this approximation, the condensate plus thermal-atom system can be characterized as a collection of noninteracting quasiparticles plus a condensate vacuum [7].

In this paper we investigate the linear and nonlinear response of such a system to vibrational perturbations of the trapping potential. If the condensate is perturbed by a weak, harmonic driving field applied at the end of the evaporative cooling cycle, the response of the condensate to the perturbation is maximal when the frequency of the driving field equals one of the quasiparticle mode energies. This is the case because the equations that determine the normal modes and frequencies of the time-dependent Ginzburg-Pitaevskii-Gross or nonlinear Schrödinger equation (NLSE) also determine the quasiparticle mode energies and field operator within the Bogoliubov approximation. This distortion of the condensate occurs because shaking the trap causes atoms to leave the condensate with the concomitant creation of new quasiparticles (quasiparticles do not correspond directly with the thermal atoms, however). These processes will be most efficient when the trap is resonantly shaken, which, in turn, causes the maximum disturbance of the condensate. We propose an experiment for measuring the quasiparticle mode energies. We also present a numerical method for computing the quasiparticle spectrum and give results for an illustrative case.

While the linear-response theory provides a precise and relatively quick method for finding the excitation frequencies, one has to consider how well it can describe the response of a real, trapped condensate. Linear-response theory assumes that the excitations do not affect the condensate ground state or couple to one another and thus may ignore a wide range of possible nonlinear effects. Furthermore, the time-dependent behavior of an excited condensate will likely be of interest in future experiments.

We have therefore also modeled the response of BEC to perturbations in the trapping potential by solving the *time-dependent* NLSE by direct numerical integration. This analysis verifies the linear-response spectrum for vibrational excitations of a radially symmetric condensate described above and, in addition, includes nonlinear effects such as the generation of harmonics of the probe frequency and frequency mixing between the resonance frequencies. Many aspects of this condensate nonlinear response should be straightforward to study in evaporatively cooled samples of alkali at-

 

oms. These phenomena are, in fact, the matter-wave analogs of conventional nonlinear optics.

## II. CONDENSATE LINEAR RESPONSE

### A. Connecting the quasiparticle spectrum and the condensate linear response

In this section we demonstrate that, if a weak, harmonic perturbation is added to the trap potential at the end of the evaporative cooling cycle, then the perturbing frequencies at which the condensate response is maximal are identical to the quasiparticle spectrum under conditions of the Bogoliubov approximation. We also describe an experiment for measuring the spectrum that can be performed on current-generation condensates. In an actual experiment, it will be very difficult to drive the condensate so as to obtain only the linear response. In practice, the condensate response will likely be nonlinear when driven on resonance. This nonlinear response will be *maximal*, however, at the linear excitation frequencies and this is the basis for the proposed experiment.

#### *1. The quasiparticle spectrum*

Consider the many-atom system whose temperature is well below the condensation point and that is composed of a condensate plus thermal atoms. We assume that most of the atoms are in the condensate and that the atom-atom interaction can be represented by a pseudopotential whose strength is determined by an $s$-wave scattering length $a$:

$$V(\mathbf{r}-\mathbf{r}')=U_0\delta(\mathbf{r}-\mathbf{r}'), \tag{2.1}$$

where

$$U_0=\frac{4\pi\hbar^2 a}{m}. \tag{2.2}$$

The grand canonical, many-atom Hamiltonian is written in terms of the boson field operator as

$$\begin{aligned}\hat{K}=&\int d^3r\,\hat{\psi}\dagger(\mathbf{r})H_0\hat{\psi}(\mathbf{r})\\&+\frac{1}{2}U_0\int d^3r\,\hat{\psi}\dagger(\mathbf{r})\hat{\psi}\dagger(\mathbf{r})\hat{\psi}(\mathbf{r})\hat{\psi}(\mathbf{r})\\&-\mu\int d^3r\,\hat{\psi}\dagger(\mathbf{r})\hat{\psi}(\mathbf{r}),\end{aligned} \tag{2.3}$$

where $H_0$ is the bare-trap Hamiltonian

$$H_0=-\frac{\hbar^2}{2m}\nabla^2+V_{\mathrm{trap}}(\mathbf{r}), \tag{2.4}$$

$\mu$ is the chemical potential, $m$ is the mass of the trapped atom, and $V_{\mathrm{trap}}(\mathbf{r})$ is the harmonic trap potential.

The boson field operators $\hat{\psi}^\dagger(\mathbf{r})$ and $\hat{\psi}(\mathbf{r})$, respectively, create and destroy an atom at position $\mathbf{r}$ and satisfy the commutation relations

$$\begin{aligned}&[\hat{\psi}(\mathbf{r}),\hat{\psi}^\dagger(\mathbf{r}')]=\delta(\mathbf{r}-\mathbf{r}'),\\&[\hat{\psi}(\mathbf{r}),\hat{\psi}(\mathbf{r}')]=[\hat{\psi}^\dagger(\mathbf{r}),\hat{\psi}^\dagger(\mathbf{r}')]=0.\end{aligned} \tag{2.5}$$

Under the Bogoliubov approximation, the condensate is assumed to contain most of the atoms so that $N-N_0\ll N_0$, where $N_0$ denotes the macroscopic occupation of the condensate and $N$ denotes the total number of condensate plus thermal atoms. In this case, the field operator can be written as the sum of a $c$-number *condensate wave function* $\Psi(\mathbf{r})$ plus a small correction $\hat{\phi}(\mathbf{r})$,

$$\hat{\psi}(\mathbf{r})=\Psi(\mathbf{r})+\hat{\phi}(\mathbf{r}), \tag{2.6}$$

where $\Psi(\mathbf{r})$ satisfies the normalization condition

$$\int d^3r|\Psi(\mathbf{r})|^2=N_0. \tag{2.7}$$

Inserting Eq. (2.6) into Eq. (2.3) and neglecting terms in $\hat{\phi}(\mathbf{r})$ higher than quadratic yields the following expression for $\hat{K}$:

$$\begin{aligned}\hat{K}=&\int d^3r\Psi^*(\mathbf{r})\left[H_0-\mu+\frac{1}{2}U_0|\Psi(\mathbf{r})|^2\right]\Psi(\mathbf{r})\\&+\int d^3r\Psi^*(\mathbf{r})[H_0-\mu+U_0|\Psi(\mathbf{r})|^2]\hat{\phi}(\mathbf{r})\\&+\int d^3r\hat{\phi}^\dagger(\mathbf{r})[H_0-\mu+U_0|\Psi(\mathbf{r})|^2]\Psi(\mathbf{r})\\&+\int d^3r\hat{\phi}^\dagger(\mathbf{r})[H_0-\mu+2U_0|\Psi(\mathbf{r})|^2]\hat{\phi}(\mathbf{r})\\&+\frac{1}{2}U_0\int d^3r\hat{\phi}^\dagger(\mathbf{r})[\Psi(\mathbf{r})]^2\hat{\phi}^\dagger(\mathbf{r})+\frac{1}{2}U_0\int d^3r\hat{\phi}(\mathbf{r})\\&\times[\Psi^*(\mathbf{r})]^2\hat{\phi}(\mathbf{r}).\end{aligned}$$

The first term in the above equation is a $c$ number and the second and third terms will vanish identically if $\Psi(\mathbf{r})$ satisfies the time-independent NLSE [8]

$$[H_0+U_0|\Psi(\mathbf{r})|^2]\Psi(\mathbf{r})=\mu\Psi(\mathbf{r}). \tag{2.8}$$

The Bogoliubov-approximate grand canonical Hamiltonian then takes the form

$$\begin{aligned}\hat{K}_B=&\zeta'+\int d^3r\hat{\phi}^\dagger(\mathbf{r})[H_0-\mu+2U_0|\Psi(\mathbf{r})|^2]\hat{\phi}(\mathbf{r})\\&+\frac{1}{2}U_0\int d^3r\hat{\phi}^\dagger(\mathbf{r})[\Psi(\mathbf{r})]^2\hat{\phi}^\dagger(\mathbf{r})+\frac{1}{2}U_0\int d^3r\hat{\phi}(\mathbf{r})\\&\times[\Psi^*(\mathbf{r})]^2\hat{\phi}(\mathbf{r}),\end{aligned} \tag{2.9}$$

where $\zeta'$ is a $c$ number.

The Bogoliubov Hamiltonian is a sum of a quadratic form and a $c$ number and can be cast into the form of a collection of noninteracting quasiparticles by the Bogoliubov transformation

$$\hat{\phi}(\mathbf{r})=\sum_{\lambda}\left[u_{\lambda}(\mathbf{r})\beta_{\lambda}+v_{\lambda}^{*}(\mathbf{r})\beta_{\lambda}^{\dagger}\right] \tag{2.10}$$

and

$$\hat{\phi}^{\dagger}(\mathbf{r})=\sum_{\lambda}\left[u_{\lambda}^{*}(\mathbf{r})\beta_{\lambda}^{\dagger}+v_{\lambda}(\mathbf{r})\beta_{\lambda}\right], \tag{2.11}$$

where the $\beta_{\lambda}$ are quasiparticle creation and destruction operators and the implicit assumption is made that the condensate wave function is not included in the sum (we shall show later that the condensate wave function forms a special solution of the equations that $u_{\lambda}$ and $v_{\lambda}$ must satisfy). The quasiparticle operators satisfy the usual commutation relations for boson creation and destruction operators

$$[\beta_{\lambda},\beta_{\lambda'}^{\dagger}]=\delta_{\lambda\lambda'},\quad [\beta_{\lambda},\beta_{\lambda'}]=[\beta_{\lambda}^{\dagger},\beta_{\lambda'}^{\dagger}]=0. \tag{2.12}$$

The reduction of $\hat{K}_B$ to a collection of noninteracting quasiparticles occurs if the $u_{\lambda}$ and $v_{\lambda}$ satisfy the equations

$$\mathcal{L}u_{\lambda}(\mathbf{r})+U_0[\Psi(\mathbf{r})]^2v_{\lambda}(\mathbf{r})=E_{\lambda}u_{\lambda}(\mathbf{r}) \tag{2.13}$$

and

$$\mathcal{L}v_{\lambda}(\mathbf{r})+U_0[\Psi^{*}(\mathbf{r})]^2u_{\lambda}(\mathbf{r})=-E_{\lambda}v_{\lambda}(\mathbf{r}), \tag{2.14}$$

where

$$\mathcal{L}=H_0-\mu+2U_0|\Psi(\mathbf{r})|^2 \tag{2.15}$$

and the $u_{\lambda}$ and $u_{\lambda}$ are square-integrable functions. The form of the Bogoliubov-approximate grand canonical Hamiltonian after performing this transformation is, to within a $c$ number,

$$\hat{K}_B=\sum_{\lambda}E_{\lambda}\beta_{\lambda}^{\dagger}\beta_{\lambda}. \tag{2.16}$$

The details of deriving the above form are contained in Ref. [7]. Note, however, that the definition of the $v_{\lambda}$ in this paper differs by a sign change from those contained in that reference.

This is a Hamiltonian describing a collection of noninteracting quasiparticles for which the condensate is the vacuum. The condensate wave function and the quasiparticle mode spectrum can therefore be completely determined by solving the system of coupled equations

$$[H_0+N_0U_0|\psi_g(\mathbf{r})|^2]\psi_g(\mathbf{r})=\mu\psi_g(\mathbf{r}), \tag{2.17}$$

$$\mathcal{L}u_{\lambda}(\mathbf{r})+N_0U_0[\psi_g(\mathbf{r})]^2v_{\lambda}(\mathbf{r})=E_{\lambda}u_{\lambda}(\mathbf{r}), \tag{2.18}$$

$$\mathcal{L}v_{\lambda}(\mathbf{r})+N_0U_0[\psi_g^{*}(\mathbf{r})]^2u_{\lambda}(\mathbf{r})=-E_{\lambda}v_{\lambda}(\mathbf{r}), \tag{2.19}$$

where we have written the condensate wave function as $\Psi(\mathbf{r})=N_0^{1/2}\psi_g(\mathbf{r})$ to make explicit the number of condensate atoms.

### *2. The condensate linear response to weak perturbation of the trap potential*

Next we consider the effect of applying a weak, sinusoidal perturbation to the trap potential that confines the equilibrium system described above. Applying such a perturbation will cause the condensate to oscillate and its deformed shape can be detected. The key to the connection between the quasiparticle spectrum and the condensate linear response is that the effect of the small thermal-atom component on the large condensate can be neglected. Experimentally, the thermal-atom component can be made smaller and smaller (using evaporative cooling) without affecting the size of the condensate linear response. Eventually, the system can be brought to a state where the linear response, even though it is small, will dominate the effect of the thermal-atom component on the condensate. The linear-response behavior of the condensate (for $T\ll T_c$) should then be well described by the time-dependent, driven NLSE [4]

$$i\hbar\frac{\partial\Psi}{\partial t}=[H_0+U_0|\Psi(\mathbf{r},t)|^2+f_{+}(\mathbf{r})e^{-i\omega_p t}+f_{-}(\mathbf{r})e^{i\omega_p t}]\times\Psi(\mathbf{r},t). \tag{2.20}$$

The $f_{\pm}(\mathbf{r})$ are the (possibly spatially dependent) amplitudes of the sinusoidal perturbation and $\omega_p$ is the probe frequency.

To find the linear response of the condensate to the driving field, we shall assume that $\Psi(\mathbf{r},t)$ takes the form of a sum of an undisturbed ground-state part and a response part that oscillates at frequencies $\pm\omega$ as

$$\Psi(\mathbf{r},t)=e^{-i\mu t/\hbar}[N_0^{1/2}\psi_g(\mathbf{r})+u(\mathbf{r})e^{-i\omega_p t}+v^{*}(\mathbf{r})e^{i\omega_p t}]. \tag{2.21}$$

Here $\mu$ is interpreted as the chemical potential of the undisturbed ground state, which is represented by the (scaled) condensate orbital $\psi_g(\mathbf{r})$. The functions $u(\mathbf{r})$ and $v(\mathbf{r})$ are the Fourier components of the condensate's linear response to the external disturbance that oscillate at frequencies $\pm\omega_p$.

After inserting Eq. (2.21) into (2.20), retaining only terms up to first order in $u(\mathbf{r})$, $v(\mathbf{r})$, and $f_{\pm}$ and equating like powers of $e^{\pm i\omega_p t}$, three equations result that must be simultaneously solved for $\psi_g(\mathbf{r})$, $u(\mathbf{r})$, $v(\mathbf{r})$, and $\mu$. These equations have the form

$$[H_0+N_0U_0|\psi_g(\mathbf{r})|^2]\psi_g(\mathbf{r})=\mu\psi_g(\mathbf{r}), \tag{2.22}$$

$$[H_0-(\mu+\hbar\omega_p)+2N_0U_0|\psi_g(\mathbf{r})|^2]u(\mathbf{r})+N_0U_0[\psi_g(r)]^2v(\mathbf{r})=-N_0^{1/2}f_{+}(\mathbf{r})\psi_g(\mathbf{r}), \tag{2.23}$$

$$[H_0-(\mu-\hbar\omega_p)+2N_0U_0|\psi_g(\mathbf{r})|^2]v(\mathbf{r})+N_0U_0[\psi_g^{*}(\mathbf{r})]^2u(\mathbf{r})=-N_0^{1/2}f_{-}(\mathbf{r})\psi_g(\mathbf{r}). \tag{2.24}$$

These coupled equations were used for example by Pitaevskii in his treatment of the elementary excitations around a vortex [6]. They are found in a very wide range of theory and amount to the $T=0$ version of the random-phase approximation for a finite system [7]. The second-quantized version of this theory is discussed by Lee and Gunn [9], who were considering Bose condensation in a random inhomogeneous medium (e.g., vycor glass).

The condensate linear-response equations [Eqs. (2.23) and (2.24)] can be solved by writing their solution as an expansion in the condensate normal modes. We shall next develop the equations that determine these modes and show how they are used to find the linear-response solution. Most impor-

tantly, however, we will see that the normal-mode equations are identical to Eqs. (2.18) and (2.19) that define the quasiparticle mode energies.

#### *3. Normal-mode solution of the linear-response equations*

To find the normal modes of the condensate, we first set $f_{\pm}(\mathbf{r})$ to zero in Eqs. (2.23) and (2.24). It is clear that the resulting equations will support square-integrable solutions only for discrete values of $\omega_p$ (i.e., $\omega_\lambda$). The normal-mode equations thus have the form

$$[\mathcal{L}-\hbar\omega_\lambda]u_\lambda(\mathbf{r})+N_0U_0[\psi_g(\mathbf{r})]^2v_\lambda(\mathbf{r})=0 \quad (2.25)$$

and

$$N_0U_0[\psi_g^*(\mathbf{r})]^2u_\lambda(\mathbf{r})+[\mathcal{L}+\hbar\omega_\lambda]v_\lambda(\mathbf{r})=0, \quad (2.26)$$

where $\lambda$ represents a set of quantum numbers. These equations are identical to Eqs. (2.18) and (2.19) if $E_\lambda=\hbar\omega_\lambda$. To complete the connection between the quasiparticle excitation spectrum and the condensate response we show below how these normal modes describe the condensate linear response.

We define a *normal mode* as the two-component object

$$\phi_\lambda(\mathbf{r})=\begin{pmatrix}u_\lambda(\mathbf{r})\\ v_\lambda(\mathbf{r})\end{pmatrix}. \quad (2.27)$$

With this definition, Eqs. (2.25) and (2.26) can be cast in the form

$$H\phi_\lambda(\mathbf{r})=\hbar\omega_\lambda\sigma_3\phi_\lambda(\mathbf{r}), \quad (2.28)$$

where

$$H=\begin{pmatrix}\mathcal{L} & V\\ V^* & \mathcal{L}\end{pmatrix}, \quad \sigma_3=\begin{pmatrix}1 & 0\\ 0 & -1\end{pmatrix}, \quad (2.29)$$

with $V(\mathbf{r})=N_0U_0\psi_g^2(\mathbf{r})$ and $\mathcal{L}$ defined by Eq. (2.15).

The $\{\phi_\lambda\}$ constitute a complete basis set [10], orthonormal with respect to the inner product, defined by

$$\langle\phi_{\lambda_1}|\phi_{\lambda_2}\rangle\equiv\int d^3r\,\phi_{\lambda_1}^\dagger(\mathbf{r})\sigma_3\phi_{\lambda_2}(\mathbf{r})=\delta_{\lambda_1\lambda_2} \quad (2.30)$$

and the dagger denotes the transposed, complex-conjugated matrix.

The linear response equations (2.23) and (2.24) can be written, using this notation, as

$$(H-\hbar\omega\sigma_3)\psi(\mathbf{r})=-\sigma_3g(\mathbf{r}), \quad (2.31)$$

where

$$\psi(\mathbf{r})=\begin{pmatrix}u(\mathbf{r})\\ v(\mathbf{r})\end{pmatrix}, \quad g(\mathbf{r})=\begin{pmatrix}N_0^{1/2}f_+(\mathbf{r})\psi_g(\mathbf{r})\\ -N_0^{1/2}f_-(\mathbf{r})\psi_g(\mathbf{r})\end{pmatrix}. \quad (2.32)$$

The solution of the linear-response equations is found by expanding both $\psi(\mathbf{r})$ and $g(\mathbf{r})$ in the normal modes

$$\psi(\mathbf{r})=\sum_\lambda c_\lambda\phi_\lambda(\mathbf{r}), \quad g(\mathbf{r})=\sum_\lambda g_\lambda\phi_\lambda(\mathbf{r}), \quad (2.33)$$

where the $g_\lambda$ are given by the overlap integral

$$g_\lambda=\int d^3r\,\phi_\lambda^\dagger(\mathbf{r})\sigma_3g(\mathbf{r}). \quad (2.34)$$

Substituting these expansions into Eq. (2.31) yields a system of completely uncoupled equations to be solved for the $c_\lambda$. The final solution is written as

$$\psi(\mathbf{r})=-\sum_\lambda \frac{g_\lambda/\hbar}{\omega_\lambda-\omega}\phi_\lambda(\mathbf{r}). \quad (2.35)$$

Note that the *linear response* diverges when the condensate is driven exactly on resonance. This unphysical behavior results from our neglect of loss processes and nonlinear effects. The actual condensate on-resonance response is very sensitive to nonlinear effects, as will be seen later in this paper.

### B. Normal-mode solutions for an illustrative case

The problem of computing the normal modes can be cast in the form of a generalized-eigenvalue problem within a truncated basis set of trap eigenfunctions. The numerical solution can then be found using standard techniques. In this subsection we present the results of normal-mode calculations for an illustrative experimental case (in which the trap potential is isotropic) and demonstrate their convergence as a function of basis-set size ($N_{\text{basis}}$). Details of the computational method are reported in a separate paper [11].

We have computed the normal frequencies and normal-mode solutions for the case of Cs atoms contained in a magneto-optic trap whose parameters are those of a published experimental arrangement [12], for which the ground-state solution of the NLSE has been calculated previously by both time-independent [13] and time-dependent methods [14]. The mass of a Cs atom is taken to be $m=2.2\times10^{-25}$ kg and the scattering length is taken to be $a=3.18$ nm. The value of $U_0$ from Eq. (2.2) then becomes $U_0=2.0\times10^{-51}$ J m$^3$. The potential $V_{\text{trap}}(\mathbf{r})$ is that of an isotropic harmonic oscillator with a frequency of 10 Hz. This is associated with a harmonic-oscillator length scale of $r_{\text{HO}}=(\hbar/2m\omega_{\text{trap}})^{1/2}=1.95\times10^{-6}$ m. The number of condensate atoms used in this example is $N_0=10546$ and the value of the chemical potential is $\mu=4.3\hbar\omega_{\text{trap}}$.

Table I lists the $l=0$ normal frequencies for the above case where 10, 20, and 40 basis-set elements have been used. Note that only 20 basis-set functions are sufficient to obtain frequencies that have converged to four significant figures. Another feature of the normal-frequency spectrum exhibited by the table is that even a small basis-set produces nearly converged normal frequencies. Only the largest-$n$ frequencies for a given set size do not match the corresponding ones found when the set size is increased. Increasing the basis-set size allows us, in effect, merely to obtain a larger portion of the infinite normal-frequency spectrum. This aspect of the convergence of the normal frequencies with respect to basis-set size occurred for all angular momenta for which frequencies were obtained (up to $l=10$).

Table II contains the lowest ten normal frequencies for $l=0,\ldots,4$. Twenty basis-set wave functions were used in the calculation of all values and each value was rounded so as to match the value obtained when 40 wave functions were used. The frequencies given in the table are expressed in units of $\omega_{\text{trap}}$. These normal frequencies were also verified

TABLE I. Excitation frequencies as a function of basis-set size, for the atom trap parameters given in Sec. II B. The frequencies are given as multiples of the trap frequency, $\omega_{\text{trap}}$. Only the positive excitation frequencies are listed and the eigenvalue for the spurious state has been omitted. Note that the last two frequencies in each column are unreliable because of the truncated basis.

| $n$ (radial quantum number) | $N_{\text{basis}}=10$ | $N_{\text{basis}}=20$ | $N_{\text{basis}}=40$ |
|---|---|---|---|
| 1 | 2.199 | 2.193 | 2.193 |
| 2 | 3.879 | 3.873 | 3.872 |
| 3 | 5.839 | 5.598 | 5.598 |
| 4 | 9.175 | 7.384 | 7.383 |
| 5 | | 9.208 | 9.207 |
| 6 | | 11.07 | 11.06 |
| 7 | | 12.98 | 12.95 |
| 8 | | 14.89 | 14.85 |
| 9 | | 18.46 | 16.76 |
| 10 | | | 18.69 |
| 11 | | | 20.62 |
| 12 | | | 22.57 |
| 13 | | | 24.52 |
| 14 | | | 26.47 |
| 15 | | | 28.43 |
| 16 | | | 30.40 |
| 17 | | | 32.36 |
| 18 | | | 34.36 |
| 19 | | | 37.63 |

by solving the time-dependent NLSE in the limit of weak driving. This is described in Sec. III.

The main result of the condensation is the appearance of elementary excitations with frequencies shifted away from that of the uncondensed atoms in the trap. This shift is illustrated in Fig. 1, which contains a plot of $\omega_{n00}$ for $n=1,\ldots 7$ as a function of $\beta=\mu/\hbar\omega_{\text{trap}}$. This shift in frequency is a very convenient observable for experiments that rely on laser cooling and trapping techniques where the translational motion of the atoms can be easily observed. Note that the $\omega_{nlm}$ in the figure are referenced to $\beta$ and that both the vertical and horizontal scales are graduated in units of $\hbar\omega_{\text{trap}}$. The dotted horizontal lines indicate the excitation frequencies of the bare-trapping potential.

### C. The proposed experiment

It is possible to measure directly the quasiparticle excitation of a condensate–thermal-atom system whose condensate fraction is large ($\sim$90%) and whose temperature is well below the transition point ($T\ll T_c$). The steps that would be performed are as follows. First, evaporatively cool the atoms until the number of condensate atoms is much larger than the number of thermal atoms. Second, apply a very weak harmonic perturbation to the trapping potential at probe frequency $\omega_p$ at the end of the cooling cycle. Next, probe the condensate shape (e.g., allow the condensate to expand ballistically and take a flash picture). Finally, repeat the above steps with an incremented value of $\omega_p$ until the maximum distortion of the condensate (relative to the case where no perturbation was applied) is found.

In practice, the number of condensate atoms will vary from shot to shot so that the resonance lines will be blurred somewhat. For the time-averaged orbiting potential trap of Ref. [1] this should amount to no more than 10% [15], and it is possible to collect cloud images for many condensates that

TABLE II. Lowest ten positive normal frequencies, in units of $\omega_{\text{trap}}$, for $l=0$–4, for the atom trap parameters given in Sec. II B.

| $n$ (radial quantum number) | $l=0$ | $l=1$ | $l=2$ | $l=3$ | $l=4$ |
|---|---|---|---|---|---|
| 0 | 0.000 | 1.000 | 1.526 | 2.065 | 2.660 |
| 1 | 2.193 | 2.872 | 3.510 | 4.156 | 4.828 |
| 2 | 3.872 | 4.636 | 5.373 | 6.104 | 6.844 |
| 3 | 5.598 | 6.422 | 7.223 | 8.014 | 8.807 |
| 4 | 7.383 | 8.244 | 9.088 | 9.921 | 10.75 |
| 5 | 9.207 | 10.10 | 10.97 | 11.83 | 12.69 |
| 6 | 11.06 | 11.97 | 12.87 | 13.76 | 14.64 |
| 7 | 12.95 | 13.87 | 14.78 | 15.69 | 16.59 |
| 8 | 14.85 | 15.78 | 16.71 | 17.63 | 18.54 |
| 9 | 16.76 | 17.71 | 18.64 | 19.57 | 20.49 |

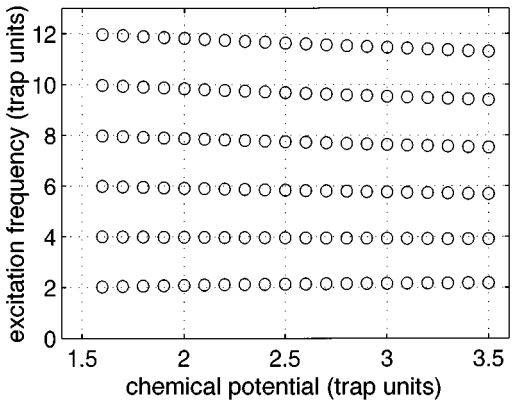


FIG. 1. Plot of the lowest seven excitation frequencies (excluding the spurious state) for the case $l=m=0$ as a function of ground-state energy (chemical potential expressed in units of $\hbar\omega_{\rm trap}$).

are all perturbed by the same frequency while simultaneously measuring the condensate fraction. The cloud images could then be binned so that only systems with the same condensate fractions could be compared.

A related experiment can also be performed to measure the damping time of the quasi-particle modes directly in the time domain. Once the mode energies have been measured, a single mode can be excited by applying the perturbation at the proper frequency and following the mode's decay by probing after successively longer delay times. These experiments may, however, be affected by two- and three-body inelastic scattering processes for long delay times [15].

## III. CONDENSATE NONLINEAR RESPONSE

### A. Solving the time-dependent NLSE

To study the general nonlinear response of the condensate to external probes we have solved the time-dependent, driven NLSE by direct numerical integration. For this purpose, we write the NLSE in the form

$$i\hbar\,\frac{\partial\psi(\mathbf{r},t)}{\partial t}=\left[-\frac{\hbar^2}{2m}\,\nabla^2+\frac{1}{2}\,m\omega_{\rm trap}^2 r^2+N_0U_0|\psi(\mathbf{r},t)|^2+V_p(\mathbf{r},t)\right]\psi(\mathbf{r},t), \tag{3.1}$$

where $V_p(\mathbf{r},t)$ represents an arbitrary time-dependent probe.

We consider only radially symmetric solutions and write the radial part of the wave function in the form

$$\psi(r)=A\,\frac{\phi(r)}{r}, \tag{3.2}$$

where $A$ is a constant used to ensure proper normalization. With this substitution and the transformation to harmonic-oscillator units

$$\rho=\left(\frac{\hbar}{2m\omega_{\rm trap}}\right)^{-1/2} r,\quad \tau=\omega_{\rm trap}t \tag{3.3}$$

the three-dimensional (3D) NLSE becomes an effectively 1D equation

$$i\,\frac{\partial\phi(\rho,\tau)}{\partial\tau}=\left[-\frac{\partial^2}{\partial\rho^2}+\frac{1}{4}\,\rho^2+8A^2N_0\pi a\,\frac{|\phi(\rho,\tau)|^2}{\rho^2}+V_p(\rho,\tau)\right]\phi(\rho,\tau). \tag{3.4}$$

Because $N_0$ appears as part of the nonlinear potential, we require the norm of $\psi(\mathbf{r})$ to be one, i.e.,

$$4\pi\left(\frac{\hbar}{2m\omega_{\rm trap}}\right)^{1/2}A^2\int_0^\infty|\phi(\rho,\tau)|^2d\rho=1. \tag{3.5}$$

During our calculations, we maintain a normalization of $\int_0^\infty|\phi(\rho)|^2d\rho=1$. This means that the values of the nonlinear coefficient that we quote are for $C_{\rm NL}=2N_0a(2m\omega_{\rm trap}/\hbar)^{1/2}$ in order to satisfy Eq. (3.5).

We begin with ground-state condensate wave functions, which can be found using a number of methods [13,14]. We then apply the NLSE to these solutions and propagate them through time using the Crank-Nicolson numerical method for diffusive, initial value, partial differential equations [16]. At each time step, we can change the value of $V_p$ in order to simulate a time-dependent probe.

One of our aims is to determine the excitation resonance frequencies, that is, those frequencies at which the condensate responds most strongly to the probe and compare these with those determined by the linear-response theory. This frequency response spectrum can be found directly from the time-dependent wave function as follows. At each time step we record the value of the wave function at a given spatial point. The resulting array provides a map of the condensate's motion as a function of time. It describes the temporal response of the condensate, and as such, may be Fourier transformed to yield a spectrum of the frequencies at which various components of the condensate are oscillating. This spectrum thus shows the frequencies of the vibrational excitations on the condensate. We will discuss its characteristics in more detail later on.

### B. Weak-probe response

First, consider a weak, single-frequency probe of the form

$$V_p=K\,\cos(k_p\rho-\omega_p\tau), \tag{3.6}$$

where $k_p$ and $\omega_p$ are the probe wave number and frequency, respectively, and $K$ is the amplitude. By varying $\omega_p$ and monitoring the response of the wave function, we are able to determine the condensate's resonance frequencies using the Fourier transform method described above. In general, a probe will most efficiently drive a given resonance (identified by the index $\lambda$) if $\omega_p$ and $k_p$ match well with $\omega_\lambda$ and $k_\lambda$, respectively. However, we find that the location of the peaks in the excitation spectrum has virtually no dependence on the probe wave number. Thus we set $k_p=1$ in all cases described in this section.

In order to compare the results of this method to those from the linear-response theory, we apply a very weak probe. By weak we mean that $K$ is much less than the nonlinear coefficient. Specifically, in the examples discussed in this section, $K=0.15$ and $C_{\rm NL}=34.5$. This nonlinearity corresponds to parameters that match those used in the previous

linear-response calculations. Since the results depend only on $C_{\mathrm{NL}}$, they can be scaled to include a number of different experimental configurations, including a trap with $\omega_{\mathrm{trap}}=25$ Hz and containing 4400 $^{87}$Rb atoms. (For $^{87}$Rb, $a\approx 6$ nm [17].)

When $\omega_p$ matches one of the resonance frequencies listed in the $l=0$ column of Table II, $\omega_\lambda$, the frequency response spectrum shows marked differences from the off-resonance case. Figure 2(a) shows the off-resonance response, for $\omega_p=1.8$, and for an integration time of $\tau=50$. [Unless otherwise noted, all times, frequencies, and wave numbers are quoted in harmonic-oscillator trap units, as defined in Eq. (3.3).] The vast majority of the response appears at zero frequency, which corresponds to the ground vibrational state of the trap. We interpret the relative strength of this peak as an indication that very little of the condensate has been excited into higher vibrational modes. Only a very weak response is visible at the probe frequency and also at the first resonance frequency $\omega_1\approx 2.2$. However, when $\omega_p=\omega_1$, significant excitation of the condensate occurs, as shown in Fig. 2(b). In this case, spectral features corresponding to the ground state and to the first excited mode appear with nearly equal intensities. This suggests that the the first excited mode has a population similar to the ground state. The other peaks in the spectrum are at integer multiples of $\omega_1$: they are harmonics of the probe and will be discussed in more detail in Sec. III C.

This distinctive behavior allows us to identify the resonance frequencies fairly straightforwardly. The first six excited modes, as determined with this method, are $\omega_1=2.20(6)$, $\omega_2=3.90(6)$, $\omega_3=5.67(6)$, $\omega_4=7.35(6)$, $\omega_5=9.22(6)$, and $\omega_6=11.10(6)$. These agree to within uncertainty to the radially symmetric (i.e., $l=0$) excitation frequencies listed in Table II. The normal modes method is, of course, limited to weak response, but is capable of much higher precision with less computational effort than the technique presented in this section. The method just outlined requires a fairly time-consuming search through various values of $\omega_p$ in search of resonances, which in turn must be identified somewhat subjectively from the response spectra. Furthermore, the resolution of the Fourier transform is determined by the propagation time of the simulation: high resolution requires long integration times.

We turn now to a brief discussion of these linear excitations. Figure 3 shows the condensate wave function in its ground state (dashed line) and after the application of a probe with frequency $\omega_p=7.35$ for $\tau=25$ (solid line.) The excitations are clearly visible as radial density variations on the ground-state background.

The excitation frequencies show a distinct difference from those expected for the noninteracting case, that is, from uncondensed atoms in a 3D harmonic trap. In that case, the vibrational energy levels are well known to be separated by $\hbar\omega_{\mathrm{trap}}$. However, in the case of radially symmetric (zero angular momentum) solutions, excitations are only allowed between alternating energy levels of the harmonic oscillator. This means that the peaks in the frequency spectrum of a noninteracting oscillator are separated by $2\omega_{\mathrm{trap}}$. The results in the interacting case differ from this by up to 10%, even at the modest value of $C_{\mathrm{NL}}$ used here. These frequency shifts arise as a result of several changes in the gas following condensation. First, the speed of propagation of a disturbance on

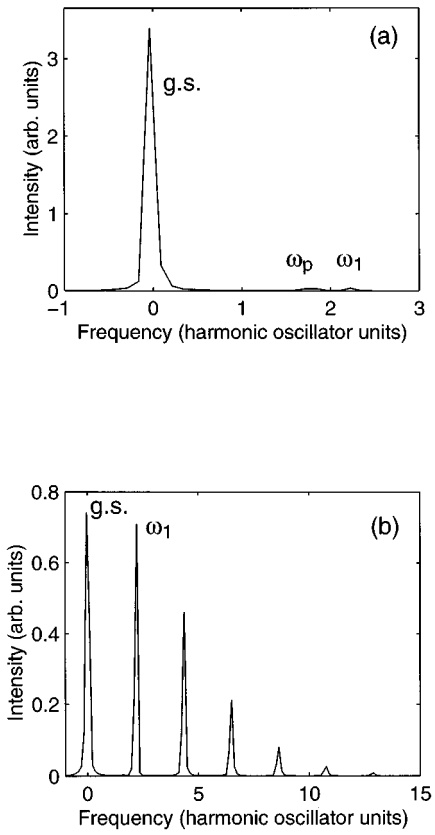


FIG. 2. Condensate response following driving with a single-frequency sinusoidal probe for $\tau=50$. (a) Response to an off-resonance probe ($\omega_p=1.8$) showing most of the condensate in the vibrational ground state, labeled g.s. The first resonance frequency is at $\omega_1$. (b) Response when $\omega_p=\omega_1$. In this case, the response at the first resonance frequency is as strong as that of the ground state, and a number of harmonics have been excited.

the condensate increases as the nonlinear term in Eq. (3.1) becomes larger [4], which in turn causes an increase in the resonance frequencies. However, as the nonlinearity increases, the condensate expands (assuming $a>0$), which tends to shift the resonance frequencies down. These considerations have different relative importances to higher- or lower-frequency excitations and indeed some of the resonances listed above are upshifted while others are downshifted from the uncondensed values (see Fig. 1).

### C. Strong-probe response

The appearance of the harmonics in Fig. 2(b) is a clear indication of a nonlinear response. This excitation of harmonics is not predicted in the linear-response theory and is significantly stronger than in a noninteracting gas. By nonlinear response we mean effects due to the coupling between the excited modes and the ground state due to the presence of condensation. Such coupling is expected as a result of the nonlinear potential in Eq. (3.1). Any perturbation in the overall potential causes a corresponding time-dependent change in the wave function. This change in the wave function in turn causes further variation in the nonlinear potential, and so on. This process can eventually lead to the population of modes with a variety of momenta and to the generation of

harmonics of the input frequency. The nonlinear response is magnified when the probe matches a resonance frequency, because in this case the initial variation in the condensate wave function is the strongest. Harmonics of the probe frequency appear even away from resonances; however, in this case they are several orders of magnitude weaker than the first order response at $\omega_p$.

A frequency response consisting of equally spaced excitations is also expected in an uncondensed harmonic oscillator, but there the physical description is qualitatively and quantitatively different from the condensed case. Because the energy level structure of the linear harmonic oscillator consists of equally spaced levels, driving the system at the proper resonance frequency, i.e., $\omega_p=2.0$, will cause transitions to the first excited level, from which excitation can occur to the second level, and so forth. These higher-order components will be very small. For a nonlinear oscillator, the energy levels are not equally spaced and so a similar process can only occur with a much lower efficiency. The equally spaced peaks in the condensate spectrum are harmonics caused by nonlinear response. We find that the excitation to higher modes is much weaker in an uncondensed system than is the production of harmonics in a condensate: the strength of the respective responses differs by a factor of about 100 for equal probe amplitudes.

To extend the results obtained above with single-frequency probe, we now consider the effects of a stronger, broadband probe. By applying a probe with a wide range of frequency components, we hope to excite a number of vibrational modes simultaneously and to observe effects due to their coupling. We drive the condensate with ''white noise'' by multiplying the trap potential by a random number between 1 and $\eta$, where $\eta$ is of order 5, at each time step. After several hundred time steps, the driving stops and the excited wave function evolves in the usual, time-independent, trap potential. During this evolution, we record the value of the wave function at a given spatial point at each time step and Fourier transform the resulting time profile as before. Because the driving process is random, we must average the results of several runs in order to get a more accurate view of the condensate response. However, the broadband method is more efficient for finding the frequency spectrum than the single-frequency technique, because all of the resonances will appear in a single computation.

Figure 4 shows an example of this response, averaged over four runs for which $\eta=3.5$ and $C_{\mathrm{NL}}=34.5$. The driving duration was $\tau=1.8$ and the unperturbed evolution time was $\tau=198.2$. During the driving time, 300 computational time steps elapsed.

A large number of excitations are visible (Fig. 4); these are identified individually in Table III. (The contribution of the ground state at zero frequency has been removed for clarity.) It is possible to identify features corresponding to the first four resonance frequencies found in Sec. III B. As in the case of the single-frequency probe, a number of harmonics of the resonance modes appear. Furthermore, features whose frequencies correspond to sums and differences of the resonances and the harmonics are also evident. This frequency mixing is a further indication that nonlinear processes are present in the condensate's response.

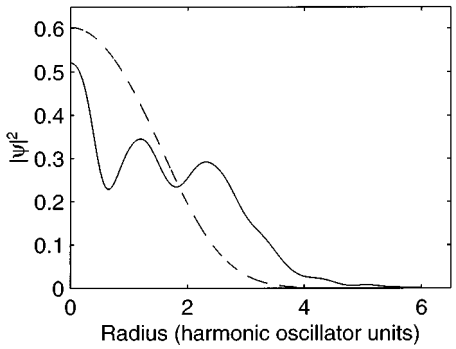


FIG. 3. The dotted line shows the wave function for a condensate in its ground state, while the solid line is the same wave function following the application of a resonant single-frequency probe ($\omega_p=7.35$). The excitation due to the probe shows up as radial density fluctuations.

The relative strengths of the spectral features in Fig. 4 merit some discussion. The maximum intensity of several of the features is beyond the scale of Fig. 4; in fact, the height of feature *b* is about 500 on this scale and the contribution of the ground state is a factor of 100 larger again. Clearly, the broadband probe is not as effective at exciting the resonance modes as is a single-frequency, on-resonance probe. Furthermore, the harmonic generation and frequency mixing processes produce responses that are relatively weak, especially at the higher frequencies. Changes to the duration of the driving stage, the size of the time step, and the value of $\eta$ have only a minor effect on the relative strengths of the various spectral features.

Both the harmonic generation and frequency mixing are the matter-wave equivalents of the corresponding processes in conventional (light) optics. The possibility of nonlinear atom optics in a number of other systems has also been proposed recently [18] and the availability of condensates adds another platform for observing such effects with coherent matter waves.

## IV. DISCUSSION

In summary, we have proposed an experiment to probe the quasiparticle mode spectrum of a system consisting of a large Bose-Einstein condensate plus a relatively smaller component of thermal atoms. This experiment consists of applying a weak, sinusoidal perturbation to the trap potential at the end of the evaporative cooling cycle and then measuring the disturbance this produces on the condensate relative to the case where no disturbance is applied. We have also demonstrated that the frequencies of the applied perturbation at which the linear response of the condensate is maximal are exactly the quasiparticle mode energies. In an actual experiment, exciting only the condensate's linear response on resonance will be very difficult due to the dominance of nonlinear effects even for very weak driving. We have seen, however, that there is a significant difference in the nonlinear condensate response between on- and off-resonance driving. The difference should serve as a clear signature of the positions of the modes in the quasiparticle spectrum.

We have also seen that it should be possible to observe nonlinear effects in the response of a dilute atomic Bose-

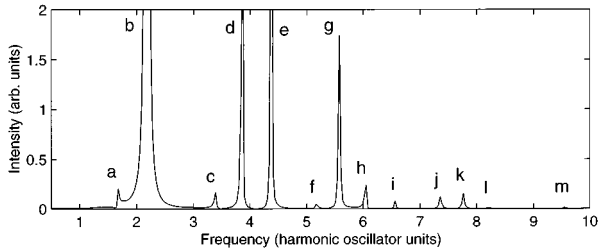


FIG. 4. Condensate response following the application of a broadband probe. The features labeled in this spectrum are identified in Table III. The first four resonance frequencies, some of their harmonics, and several sum and difference frequencies are visible. The harmonic generation and frequency mixing indicate the presence of nonlinear coupling between the vibrational modes. The contribution of the ground state at zero frequency has been subtracted from this spectrum.

Einstein condensate to even a very modest external probe. These effects are due, of course, entirely to the presence of the nonlinear mean-field term in Eq. (3.1). The experimental observation of harmonic generation or frequency mixing would therefore be a good diagnostic of the presence of a mean field.

The theoretical approach used here relies on a zero-temperature, mean-field approximation and does not include a mechanism for damping or dissipation of excitations within the condensate. We believe that a mean-field method can closely model the condensates that are currently experimentally accessible, because a similar calculation [19] has achieved a very good match with the experimental results in [1]. We should, however, address the effects of dissipation on the excitations we study. A finite excitation lifetime would mean that condensate vibrations would need to be observed fairly quickly after the probe was applied. The excitations would also acquire a frequency width inversely proportional to their lifetime. The lack of any damping means that the fundamental width of the peaks in the response spectra we present is zero, although the peaks are broadened by the imperfect resolution of the Fourier transform. In the case of the real condensates currently under experimental study, the main damping will be from two loop corrections to the mean field (i.e., collisions). This is because one loop effects such as Landau damping [20] should not be effective in a small trap. A full calculation of the two loop diagram is under way for a condensate in a trap [21], but quantitative results are not available at the moment. We know, however, that in a recent experiment [1], collisions occur at a rate of approximately 1/10 of the trap oscillation frequency [22]. The resulting damping rate should thus be small enough that it should be possible to resolve many of the features predicted here.

TABLE III. Spectral features shown in Fig. 4. All frequencies are in units of $\omega_t$. The uncertainty in the frequencies is $\pm 0.02$, and results primarily from the resolution of the Fourier transform.

| Label | Frequency | Description |
|---|---|---|
| *a* | 1.67 | $\omega_2-\omega_1$ |
| *b* | 2.19 | $\omega_1$ |
| *c* | 3.38 | $\omega_3-\omega_1$ |
| *d* | 3.86 | $\omega_2$ |
| *e* | 4.38 | $2\omega_1$ |
| *f* | 5.17 | $\omega_4-\omega_1$ |
| *g* | 5.57 | $\omega_3$ |
| *h* | 6.05 | $\omega_1+\omega_2$ |
| *i* | 6.57 | $3\omega_1$ |
| *j* | 7.36 | $\omega_4$ |
| *k* | 7.72 | $2\omega_2$ |
| *l* | 8.24 | $2\omega_1+\omega_2$ |
| *m* | 9.55 | $\omega_1+\omega_4$ |

The widths of the mode frequencies could hinder a clean measurement of the excitation spectrum. These widths will be determined by the lifetimes of the excitations caused by the applied disturbance and the lifetimes will, in turn, be limited by losses due to either interaction of the condensate with the thermal atoms or interaction of the condensate atoms with themselves. The theory we have presented in this paper does not account for these processes and indeed the condensate linear response diverges exactly at resonance.

If the lifetime of the excitation is too long, then the width of the peaks in the frequency spectrum could become more narrow than the experimental resolution. There is some degree of experimental control that can be exercised over this lifetime. If the condensate fraction is reduced, then the enhanced thermal component should limit the lifetime and thus increase the resonance widths. If the condensate fraction is too small, however, the theory presented in this paper will not be valid and a more sophisticated treatment (in which the effect of the thermal-atom component on the condensate is accounted for) must be used [23]. This can be achieved by solving the finite-*T* Hartree-Fock-Bogoliubov equations [24]. Even under the conditions assumed in this paper, the excited atoms will affect the mode energies. We expect this effect to be minimal due to the modest size of the thermal-atom component assumed. It has been shown by several authors that excited atoms merely shift and damp the quasi-particle modes as long as the condensate is not too close to the region of critical fluctuations. For the homogeneous case, the dominant damping mechanism is Landau damping of the motion of the condensate as has been shown by Payne and Griffin [20].

The elementary excitations also have characteristic shapes that will influence the efficiency with which we can drive them. This is because the coupling to a given mode will depend on the overlap of the mode with the shape of the driving potential, a fact that one can exploit in examining the dynamics of the condensate. We expect them to be long lived as soon as we are out of the narrowed region for critical fluctuations in the trap.

In order to model exactly the current generation of atomic traps, it will be necessary to extend this technique to configurations that are not spherically symmetric. Such an extension would require a full 2D or 3D treatment, but would allow us to consider rotational excitations and possibly even vortices. In addition, several recent proposals have suggested that condensates created from atoms with negative scattering lengths may be stable or metastable [13,25]. An analysis of the excitation spectra of such systems should help clarify this question and is planned to be addressed in a future paper.

**ACKNOWLEDGMENTS**

Work at Oxford was supported with funding from the Rhodes Trust and the U.K. Engineering and Physical Sciences Research Council. M.E. acknowledges funding from National Science Foundation Grant No. PHY-9612728 and also from the GSU Foundation. C.W.C. acknowledges funding from National Science Foundation Grant No. PHY-9601261. This work was supported in part by the Institute for Theoretical Atomic and Molecular Physics at Harvard University and the Smithsonian Astrophysical Observatory. The authors would like to thank Murray Holland, Eric Cornell, and Nick Proukakis for helpful discussions.

[1] M. H. Anderson, J. R. Ensher, M. R. Matthews, C. E. Wieman, and E. A. Cornell, Science **269**, 198 (1995).

[2] C. C. Bradley, C. A. Sackett, J. J. Tollett, and R. G. Hulet, Phys. Rev. Lett. **75**, 1687 (1995).

[3] K. B. Davis, M.-O. Mewes, M. R. Andrews, N. J. van Druten, D. S. Durfee, D. M. Kurn, and W. Ketterle, Phys. Rev. Lett. **75**, 3969 (1995).

[4] P. Nozières and D. Pines, *The Theory of Quantum Liquids* (Addison-Wesley, Redwood City, CA 1990).

[5] N. Bogoliubov, J. Phys. (USSR) **11**, 23 (1947).

[6] L. P. Pitaevskii, Zh. Eksp. Teor. Fiz. **40**, 646 (1961) [JETP **13**, 451 (1961)].

[7] A. L. Fetter, Ann. Phys. (N.Y.) **70**, 67 (1972); Phys. Rev. A **53**, 4245 (1996).

[8] V. L. Ginzburg and L. P. Pitaevskii, Zh. Eksp. Teor. Fiz. **34**, 1240 (1958) [Sov. Phys. JETP **7**, 858 (1958)]; E. P. Gross, J. Math. Phys. **4**, 195 (1963).

[9] D. K. K. Lee and J. M. T. Gunn, J. Phys.: Condens. Matter **2**, 7753 (1990).

[10] Jean-Paul Blaizot and Georges Ripka, *Quantum Theory of Finite Systems* (MIT Press, Cambridge, MA, 1986).

[11] R. J. Dodd, M. Edwards, C. J. Williams, C. W. Clark, P. A. Ruprecht, and K. Burnett, J. Res. Nat. Inst. Stand. Tech. (to be published).

[12] Ch. Monroe, E. Cornell, and C. Wieman, in *Laser Manipulation of Atoms and Ions*, Proceedings of the International School of Physics ''Enrico Fermi'' Course CXVIII, Varenna, 1992 edited by E. Arimondo, W. D. Phillips, and F. Strumia (North-Holland, Amsterdam, 1992).

[13] M. Edwards and K. Burnett, Phys. Rev. A **51**, 1382 (1995).

[14] P. A. Ruprecht, M. J. Holland, K. Burnett, and M. Edwards, Phys. Rev. A **51**, 4704 (1995).

[15] E. Cornell (private communication).

[16] S. E. Koonin, *Computational Physics* (Benjamin/Cummings, Menlo Park, CA, 1986); W. H. Press, B. P. Flannery, S. A. Teukolsky, and W. T. Vetterling, *Numerical Recipes in C* (Cambridge University Press, Cambridge, England, 1988).

[17] N. R. Newbury, C. J. Myatt, and C. E. Wieman, Phys. Rev. A **51**, 2680 (1995); J. R. Gardner *et al.*, Phys. Rev. Lett. **74**, 3764 (1995).

[18] G. Lenz, P. Meystre, and E. M. Wright, Phys. Rev. Lett. **71**, 3271 (1993); W. Zhang and D. F. Walls, Phys. Rev. A **49**, 3799 (1994); K. J. Schernthanner, G. Lenz, and P. Meystre, *ibid.* **51**, 3121 (1995).

[19] M. Holland and J. Cooper, Phys. Rev. A **53**, R1954 (1996).

[20] S. H. Payne and A. Griffin, Phys. Rev. B **32**, 7199 (1985).

[21] N. Proukakis (private communication).

[22] E. Cornell (private communication).

[23] The equations for the *self-consistent* Hartree-Fock-Bogoliubov method have been been derived and critiqued in a recent work by A. Griffin, Phys. Rev. B **53**, 9341 (1996).

[24] V. V. Goldman, I. F. Silvera, and A. J. Leggett, Phys. Rev. B **24**, 2870 (1981).

[25] Yu. Kagan, G. V. Shlyapnikov, and J. T. M. Walraven, Phys. Rev. Lett. **76**, 2670 (1996).